

Design and fabrication of a three-component force sensor using micromachining technology

Jongho Kim*, Yonkyu Park** and Daeim Kang**

** Division of Physical Metrology, KRISS, P.O. Box 102, Yusong-Gu, Daejeon, 305-600, South Korea

*Tel. : +82-42-868-5241, fax : +82-42-868-5249, e-mail : jhk@kriss.re.kr

Abstract

This paper describes a design methodology of a tri-axial silicon-based force sensor with square membrane by using micromachining technology (MEMS). The sensor has a maximum force range of 5 N and a minimum force range of 0.1 N in the three-axis directions. A simple beam theory was adopted to design the shape of the micro-force sensor. Also the optimal positions of piezoresistors were determined by the strain distribution obtained from the commercial finite element analysis program, ANSYS. The Wheatstone bridge circuits were designed to consider the sensitivity of the force sensor and its temperature compensation. Finally the process for microfabrication was designed using micromachining technology.

Key words : Force sensor, MEMS, Beam theory, Piezoresistor, Finite element analysis,

1. Introduction

Until now many force sensors(load cell) based on strain gage have been used to monitor the durability of bridges, buildings from the viewpoint of safety, and control material test machine and industry robot, and so on. However as some systems are now small and need high sensitivity and accuracy, a new force sensor with small size and high sensitivity, not some conventional load cells, is required to control small force precisely.

On the other hand, recently micromachining technology(MEMS: micro electro mechanical system), combining integrated circuit fabrication and micromachining fabrication, shows the possibility of development of micro force sensor similar to pressure sensor. Especially, some researchers have tried to develop a tactile sensor comprised of some force sensors for tele-operational manipulators,

intelligent robots, and haptic interfaces. These tactile sensors can detect normal forces applied on the tactile pixels for gripping force control and generate tactile images for gripping positioning and object recognition. However, in addition to acquiring tactile images and normal forces, knowledge of tangential forces is also critical for force control, and thus, three-component tactile sensors are needed.

Kane et al.[1] and Mei et al.[2] have fabricated a tactile sensor composed of some three-component force sensors with square membrane type using micromachining technology to show the possibility of realization of tactile sensor. Its fabrication is, however, not easy because of complexity of process and shape of the sensing element. Meanwhile, Wang and Beebe[3] also manufactured a micro shear force sensor with square-membrane type.

The fabrication process of sensor is simple, but the sensitivity and temperature compensation of the sensor was not considered. On the other hand, most researchers have used finite element analysis to design a sensing element with finite square-type membrane. In case of a sensing element with a circular membrane, generally, its deflection can be obtained theoretically by elasticity and thin plate theory[4], but for a finite square-type element, it is not easy to use a theoretical approach.

Thus this paper described a design methodology for three-component micro force sensor with finite square-type sensing element based on an approximate simple beam theory. Additionally the designed sensing element was verified by commercial finite element analysis software, ANSYS ver. 5.5[5]. The optimal locations of piezoresistors in membrane was determined by considering sensitivity and temperature compensation. Finally we have performed the design process for sensing element of micro force sensor based on the silicon micromachining technique.

2. Design of sensing element for micro force sensor

2.1 Design based on beam theory

Figure.1 shows a square-type sensing element of force sensor with which can measure three-component F_x , F_y , F_z . The sensing element consists of loading block and side block. Additionally the overload protection block is attached to the sensing element for protecting the force sensor, in case of subjecting to overload.

In order to obtain the deflection of membrane and its strain distribution necessary to shape design of sensing element, the square membrane, as shown in Figure.2, is assumed as four trapezoidal beam A, B, C and D. The beam length is L , the length and height of loading block being d , h_1 and the thickness of membrane being h , and the height of the overload protection block being h_2 . The loading block is assumed as a rigid body due to thick thickness against membrane of sensing

element.

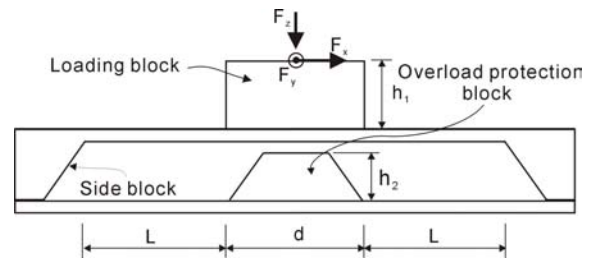


Figure.1 Schematic diagram of a sensing element subjected to F_x , F_y and F_z loadings.

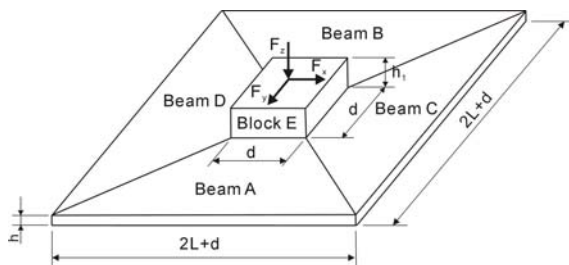


Figure.2 Schematic diagram of the trapezoidal beam model.

On the other hand, the cross beam model shown in Figure. 3 was set up to compare with the deflection and strain distribution of the trapezoidal beam model.

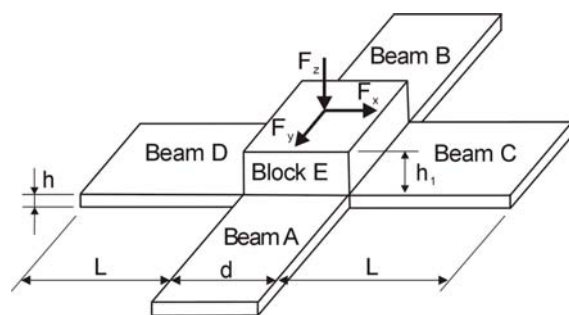


Figure.3 Schematic diagram of the cross beam model.

We used a SOI(silicon on insulator) wafer as shown in Figure. 4, which 45 μm silicon is deposited on {100} wafer with 500 μm thickness. The size of the membrane has 2.404 mm \times 2.404 mm, and its thickness being 45 μm . The capacity of each loading

is 0.1 N ~ 5 N, which is force range necessary to feeling of texture when human object touch on surface[6]. In case of {100} wafer, the supporting block of sensing element has 54.74° slope when an anisotropic wet etching using KOH solution is conducted[7]. When three loadings is applied to loading block, the maximum deflection of the trapezoidal beam model was 25.342 μm. Thus the height of the overload protection block, h_2 , is 474 μm to consider the damage of the sensing element.

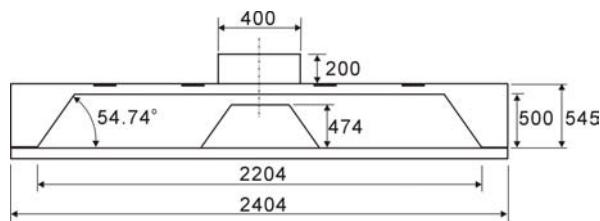


Figure.4 Schematic diagram of the dimension for the designed force sensor(unit : μm).

2.2 Finite element analysis

In order to verify the design of sensing element shown in Figure.4 using trapezoidal beam model, the commercial finite element program, ANSYS ver. 5.7, was used[5]. Figure. 5 shows the finite element model of the sensing element with eight nodes and four degrees. The supporting block of the sensing element was fixed at bottom and the each loading was assumed as concentrated force.

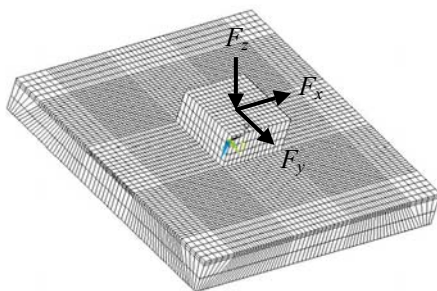


Figure.5 Finite element model of sensing element subjected to F_x , F_y and F_z loadings

On the other hand, the material properties of the silicon wafer is anisotropic. In case of {100} wafer, the components of compliance are $S_{11}=7.68 \times 10^{-3}/\text{GPa}$, $S_{12}=-2.14 \times 10^{-3}/\text{GPa}$ and

$S_{44}=12.6 \times 10^{-3}/\text{GPa}$, when rectangular coordinate is coincided with the principle axis[8]. Thus the new material properties for coordinate shown in Figure. 5 were obtained from Ting's method[9]. Additionally the analysis assumed as isotropic material has performed to compare with the result of anisotropic assumption. The properties of elastic modulus, Poisson's ratio, are 190 GPa, 0.17, respectively[7].

In case of the sensing element subjected to each loading, the strain distributions of the trapezoidal beam model were similar to those of the finite element analysis when comparing with the cross beam model[10]. On the other hand, the strain distribution of model assumed as isotropic material showed the difference of 10% compared with model assumed as anisotropic material[10]. Thus the model assumed as isotropic material could be used sufficiently, instead of anisotropic assumption, to design the sensing element made of silicon wafer.

Meanwhile Table 1 shows the comparison of maximum deflection obtained from beam theory and finite element method in case of the sensing element subjected to 5 N loading. The trapezoidal beam model was also similar to the finite element analysis against the cross beam model.

Table 1 Comparison of maximum deflection obtained from beam theory and finite element analysis under F_x , F_y and F_z loadings of 5 N.

Loading	Beam theory(μm)		FEM(μm)
	Trapezoidal	Cross	
F_z	13.910	29.726	13.803
F_x	-5.716	-2.392	-4.649
F_y	0.000	0.000	0.000

3. Design of full bridge circuit for sensitivity

The location of the piezoresistor, like strain gage, is very important from the standpoint

of sensitivity and temperature compensation of micro force sensor. Thus the optimal location of the piezoresistor was determined by the strain distribution obtained from finite element analysis. In case of square-type membrane, when the F_x or F_y loading is applied, the location of maximum strain distribution is centerline of the membrane. The location of the F_z loading is also centerline of the membrane. Thus the piezoresistors for F_x loading were away $60 \mu\text{m}$ from the centerline.

Figure.9 shows the locations of the piezoresistors corresponding to F_x , F_y and F_z loadings. Four resistors, R_{z1} , R_{z2} , R_{z3} , R_{z4} are related to F_z loading, and in case of F_x loading, R_{x1} , R_{x2} , R_{x3} , R_{x4} and in case of F_y loading, R_{y1} , R_{y2} , R_{y3} , R_{y4} are needed. The width of piezoresistor was $18 \mu\text{m}$ due to margin of the metal line.

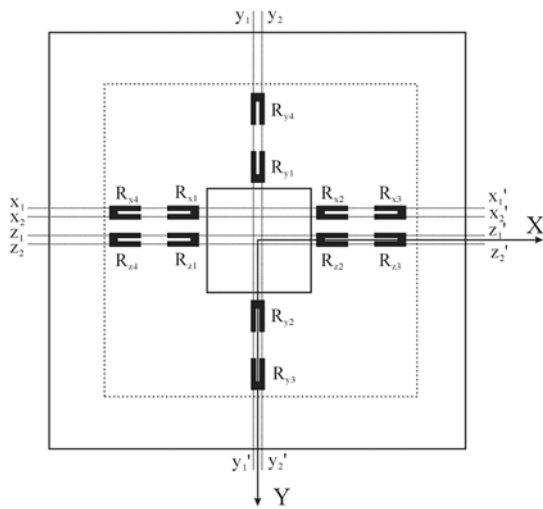


Figure.9 Location of piezoresistors for measuring F_x , F_y and F_z loadings.

In order to increase the sensitivity of the sensor and decrease the environmental temperature and coupling effects of the three-component, it is very important to set up an optimal full bridge circuit comprised of four piezoresistors. The evaluation of output voltages of three full bridge circuits corresponding to three-component loading is needed to obtain an optimal arrangement of piezoresistor within full bridge circuit to

decrease the coupling effect.

The output voltage, change rate of resistance, can be obtained simply by

$$\frac{\Delta R}{R} = K \varepsilon \quad (1)$$

, where ε is axial strain, K is gage factor. Generally, the gage factor, in case of strain gage, is 2.0, and for single silicon, 90.0 and for polysilicon, 30.0[11]. This paper has used gage factor, 90.0, due to single silicon.

The change rate, $\Delta R/R$, could be calculated easily by using strain distribution obtained from finite element analysis and equation (1). Figure.10 shows the change rate of resistance of Z_1-Z_1' , Z_2-Z_2' , X_1-X_1' , X_2-X_2' , Y_1-Y_1' and Y_2-Y_2' axis, in case of the sensing element subjected to F_z loading of 5 N. Figure.11 and Figure.12 represent the change rate of resistor of F_x or F_y loading. On the other hand, Figure.13 shows the change rate of resistor when the temperature of the sensing element increase 10°C .

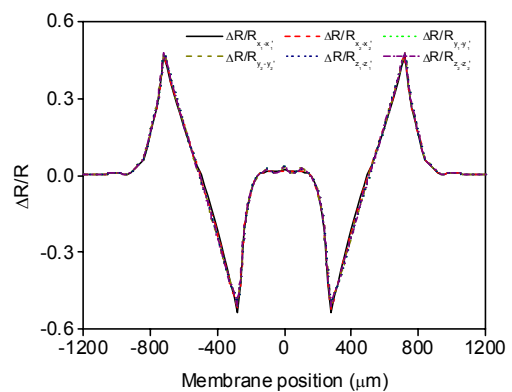


Figure.10 The rate of piezoresistors change of under F_z loading (5 N).

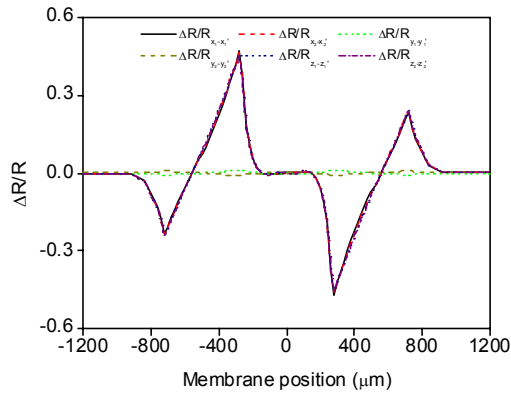


Figure.11 The rate of piezoresistors change of under F_x loading(5 N).

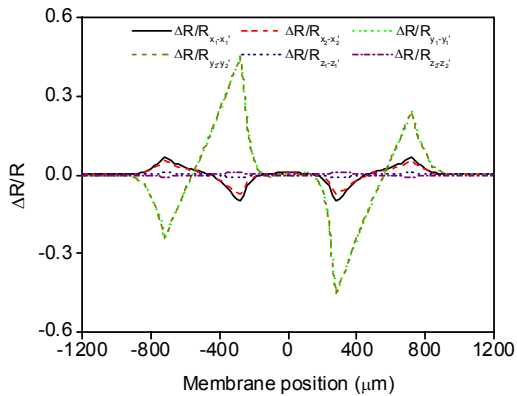


Figure.12 The rate of piezoresistors change of under F_y loading(5 N).

The optimal full bridge circuits of the three-component loading were obtained by the change rate of resistors shown in Figures 10 to 12.

Figure. 13 shows the designed full bridge circuits. In case of F_z loading, the change rate of resistor as shown in Figure. 10 is different from those of F_x and F_y loadings. Thus, in the bridge circuit of F_z loading, the arrangement of R_{z2} and R_{z3} is different from resistors of F_x and F_y circuits.

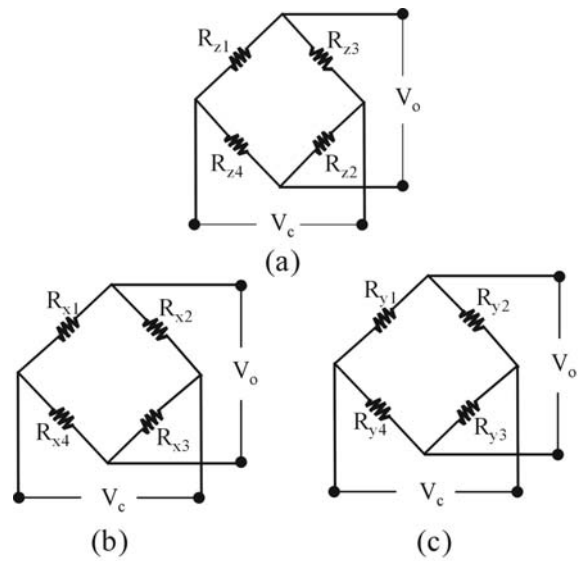


Figure. 13 Full bridge circuits of piezoresistor for measurement of three-component force : (a) F_z circuit; (b) F_x circuit; (c) F_y circuit.

Table 2 shows the output voltage obtained from full bridge circuits. The coupling effect of the three-component was almost zero. Additionally the output voltage of environmental temperature effect ($\Delta T=10$ °C) was 1/50% against the loading condition.

Table 2 Comparison of full bridge circuit output obtained from the designed force sensor under F_x , F_y and F_z loadings (5 N)

Loading	$\frac{\Delta V_o}{V_c} \Big _{F_x}$	$\frac{\Delta V_o}{V_c} \Big _{F_y}$	$\frac{\Delta V_o}{V_c} \Big _{F_z}$
F_z (5 N)	-7.78E-1	-5.55E-17	-2.78E-17
F_x (5 N)	0.00E+0	5.41E-1	0.00E+0
F_y (5 N)	0.00E+0	0.000	5.44E-1
$\Delta T=10$ °C	-2.61E-4	-5.42E-20	-8.13E-20

4. Design process of sensing element using micromaching technique

Figures.14 (a) to (e) represent the design process using micromaching technique (MEMS). The SOI wafer deposited 45 μm silicon on wafer with thickness of 500 μm is cleaned as shown in Figure.14(a). Next, in Figure. 14(b), the shape of piezoresistors

on the silicon wafer is patterned by photolithography. Figure.14(c) shows the piezoresistors created by thermal diffusion process of phosphorous. On the other hand, as shown in Figure.13, the full bridge circuits need the metal lines for connection of piezoresistors. Figure.14(d) represents the connection of contact hole and metal line using photolithography. Finally, Figure. 14(e) shows the fabricated sensing element and loading block using SU-8 photoresist and KOH solution.

Using the design process based on micromaching technique, the fabrication process is now in progress.

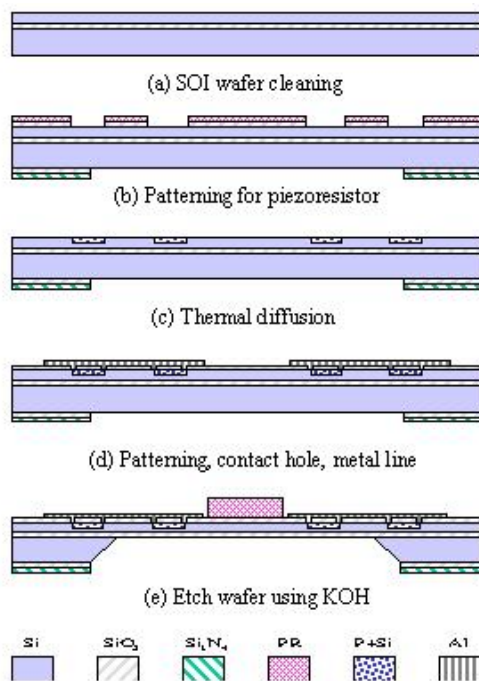


Figure. 14 Schematic diagram of micro-fabrication for tri-axial force sensor.

5. Conclusion

The micro force sensor based on micromaching technique was designed to measure three-component loading. The capacity of each loading was from 0.1 N to 5 N. In order to design the shape of the sensing element easily, the sensing element of square membrane type was simply assumed as four

trapezoidal beams. The verification using finite element analysis showed that the approximate beam theory using the trapezoidal beam model could be used efficiently in order to design the sensing element of the square membrane type. On the other hand, the optimal full bridge circuit considering the sensitivity of the sensing element, coupling effect and environmental temperature effect was designed by numerical evaluation. Finally, the design process based on micromaching fabrication was set up.

Acknowledgement

This work has been supported by the National Research Laboratory for the Force Measurement & Evaluation (Project No. 2000-N-NL-01-C-141).

Reference

1. Kane, B.J., Cutkosy, M.R. and Kovacs, G.T.A., "CMOS-compatible traction stress sensor for use in high-resolution tactile imaging," *Sensor and Actuators (A)*, Vol. 54, pp.511-516, 1996.
2. Mei, T., Li, W.J., Ge, Y., Chen, Y., Ni, L. and Chan, M.H., "An integrated MEMS three-dimensional tactile sensor with large force range," *Sensors and Actuators(A)*, Vol. 80, pp.155-162, 2000.
3. Wang, L. and Beebe, D.J., "A silicon-shear force sensor: development and characterization," *Sensor and Actuators(A)*, Vol. 84, pp.33-44, 2000.
4. Timoshenko and Woinowsky-Krieger, *Theory of plates and shells*, McGraw-Hill, Inc. 1959.
5. ANSYS Ver. 5.5 Manual, 2000.
6. Pennywitt, K. E., *Robotic tactile sensing*, in *Byte*, pp. 177-200.
7. Petersen, K.E., "Silicon as a mechanical material," *Proc. IEEE*, Vol.70, pp.420-457, 1982.
8. Wortman, J.J. and Evans, R.A., "Young's modulus, shear modulus, and Poisson's ratio in silicon and germanium," *Journal of Applied Physics*, Vol. 36(1), pp.153-156, 1965.

9. Ting, T.C.T., "Generalized Dundurs constant for anisotropic bimetals," International Journal of Solids and Structures, Vol.32, pp.483-500, 1995.

10. Kim, J.H., Cho, W.K., Park, Y.K. and Kang, D.I., " Design and fabrication of micro force sensor using MEMS fabrication technology," KSPE, Spring annual meeting, pp.497-502, 2002.

11. Mohamed, Gad-el-Hak, The MEMS Handbook, CRC Press, 2001.

Contact person for paper

Dr. Jong Ho Kim
Division of Physical Metrology, KRISS, P.O.
Box 102, Yusong-Gu, Daejeon, 305-600,
South Korea

Tel. : +82-42-868-5241

Fax : +82-42-868-5249

e-mail : jhk@kriss.re.kr